

See discussions, stats, and author profiles for this publication at: <https://www.researchgate.net/publication/44887067>

# Molecular Simulations Reveal the Mechanism and the Determinants for Ampicillin Translocation through OmpF

ARTICLE *in* THE JOURNAL OF PHYSICAL CHEMISTRY B · JULY 2010

Impact Factor: 3.3 · DOI: 10.1021/jp9110579 · Source: PubMed

---

CITATIONS

32

READS

44

## 4 AUTHORS, INCLUDING:



Amit Kumar

Università degli studi di Cagliari

28 PUBLICATIONS 185 CITATIONS

[SEE PROFILE](#)



Paolo Ruggerone

Università degli studi di Cagliari

125 PUBLICATIONS 2,076 CITATIONS

[SEE PROFILE](#)



Matteo Ceccarelli

Università degli studi di Cagliari

87 PUBLICATIONS 1,416 CITATIONS

[SEE PROFILE](#)

# Molecular Simulations Reveal the Mechanism and the Determinants for Ampicillin Translocation through OmpF

Amit Kumar, Eric Hajjar, Paolo Ruggerone, and Matteo Ceccarelli\*

Department of Physics, University of Cagliari and Istituto Officina dei Materiali/CNR UOS SLACS, I-09042 Monserrato (CA), Italy

Received: November 20, 2009; Revised Manuscript Received: April 23, 2010

We use a multiscale approach, combining molecular dynamics simulations with metadynamics, to simulate the translocation of ampicillin through OmpF from *Escherichia coli* (*E. coli*). In-depth analysis has allowed us to reveal the complete picture of the translocation process in terms of both energetics and physicochemical properties. We have demonstrated the existence of a unique affinity site at the constriction region, accessible from both sides and defined by specific pore–antibiotic interactions. By providing optimal binding, the constriction region works like an enzyme toward the permeation of ampicillin. We find reduction in entropy to be compensated by enthalpic contributions from a favorable network of interactions (hydrogen bonds and hydrophobic contacts) which is also mediated by two slow water molecules bridging the antibiotic–pore interactions. Finally, as ampicillin assumes a preferential value for a torsional angle when at the constriction region, we investigated the consequence of the conformational preorganization of ampicillin toward its translocation. As a whole, our analysis opens the way to chemical modifications of antibiotics to allow improving uptake through porins contributing to combat bacterial resistance.

## Introduction

The growing phenomena of bacterial resistance together with the simultaneous decline in research and development of new drugs is now threatening the treatment of infectious diseases.<sup>1</sup> Although antibiotic resistance involves various mechanisms, antibiotic uptake alteration is the very first defense line in Gram-negative bacteria. It is particularly difficult for hydrophilic antibiotics, such as  $\beta$ -lactams, to reach their target due to the presence of an outer membrane (OM). To cross such a barrier, antibiotics must channel through general diffusion porins, such as the outer membrane protein-F (OmpF) in *Escherichia coli*. The X-ray structure of OmpF has been solved at a high resolution (2.4 and 3.0 Å) and has revealed OmpF to be a homotrimer, where each monomer is folded as a  $\beta$ -barrel formed by 16 antiparallel  $\beta$ -strands.<sup>2,3</sup> An important feature of OmpF shown in Figure 1 is the presence of loop L3, which folds into the interior of the  $\beta$ -barrel to form a constriction region (CR). In addition to such spatial constriction, this zone is also characterized by a strong transversal electric field, generated by negatively charged residues D113, E117, and D121 (L3 side) which face a cluster of positively charged residues R42, R82, and R132 (anti-L3 side; see Figure 1). Although it is usually described as a nonspecific channel, OmpF has been shown to modulate the permeation of solutes with different sizes (~600 Da) and charges within its nanometer sized channel.<sup>4</sup> Furthermore, it has been suggested<sup>5,6</sup> that the electric field across the pore acts as a polarity separator, which facilitates permeation of polar compounds. Alteration of antibiotic permeation through porins has been described as one of the many encountered mechanism of resistance,<sup>7</sup> and our study aims at deciphering its molecular basis.

Molecular dynamics (MD) simulations have been extensively used to investigate the transport of ions and small dipolar molecules through OmpF.<sup>8,9</sup> Recent developments in algorithms and computer power promise to increase the utility of MD

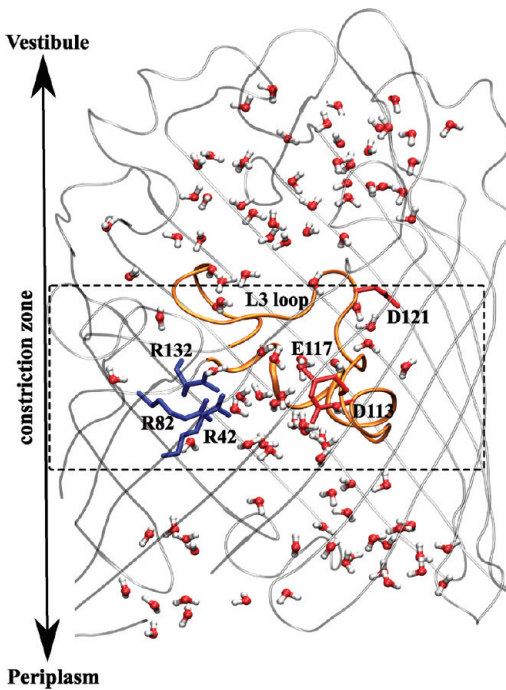


**Figure 1.** Water filled OmpF channel with our three defined regions (vestibule, constriction zone, and periplasm) is shown here (snapshot from molecular dynamics simulations). Loop L3 which folds into the channel and forms a constriction region is shown in orange, the key residues at the constriction region (basic: blue, acidic: red) is shown using licorice representation, and the water molecules are shown in ball and stick representation.

simulations to time scales over which many physiologically relevant processes take place. In our previous studies, we used the metadynamics algorithm<sup>10</sup> to study the diffusion of ampicillin and other  $\beta$ -lactam antibiotics of different sizes and charges through the OmpF channel.<sup>11,12</sup> There, we suggested the

importance of electrostatic interactions, the preferential orientation, and the role of internal coordinates of ampicillin for the translocation process. However, due to shortcomings and limitations in the methodology and analysis we used during our previous simulations, we were not able to provide the complete determinants for the translocation mechanism, which would help the rational design of antibiotics with improved permeation properties.

In the present study, we propose a multiscale approach where (1) metadynamics is used initially as an exploratory method to simulate the process of translocation and (2) from the identified free-energy minima additional simulations are performed to complete the structural and energetic pathway of translocation. In particular, we improved the methodology of simulations and analysis: (i) enhancing the sampling of conformation for ampicillin by placing it well above the constriction region, (ii) using a new reaction coordinate to explicitly account for the orientation of ampicillin, (iii) investigating the importance of water mediated interactions between ampicillin and OmpF, and (iv) identifying essential hydrogen bonds and hydrophobic interactions between ampicillin and OmpF for the translocation process. These improvements have allowed us to test whether ampicillin translocates through OmpF following the two-barrier-one-binding-site model (2B-1BS).<sup>13</sup> This analytical model assumes that the binding is a prerequisite for translocation, and though it matches well with the high rate of permeation of sugar molecules through specific channels, it is not obvious how this transfers to the permeation of antibiotics through nonspecific channels. Here, we were able to identify a unique deep affinity site for ampicillin, located at the constriction region and accessible from both sides of the channel, as shown by experiments.<sup>14</sup> Furthermore, we were able to characterize this affinity site in terms of hydrogen bonded, hydrophobic, and water-mediated interactions between ampicillin and the pore. These enthalpic terms collectively contribute to compensate the loss of entropy of the antibiotic when translocating through the narrow constriction region, recalling the entropy/enthalpy compensation of enzymatic association.<sup>15,16</sup> Furthermore, we present the results of additional simulations that clearly demonstrate the energetic consequences of preorganizing ampicillin for its diffusion across OmpF.

## Material and Methods

**Simulation Methodology.** Our model system consists of a single monomer of the trimeric crystal structure (pdb-id: 2OMF) solved at 2.4 Å resolution.<sup>2</sup> Previous MD simulations and experimental investigations have shown the independence of monomers toward the transport of ions<sup>8</sup> and small-molecules,<sup>17</sup> which justifies our choice of a single monomer. The system was prepared, as described in our previous study.<sup>11</sup> We used the AMBER force field<sup>18</sup> for OmpF monomer and TIP3P model for water and our developed parameters for the lauryl dimethyl amino oxide (LDAO) detergent and ampicillin.<sup>11,19</sup> Ampicillin was manually placed at  $z = +12$  Å from the constriction region (located at  $z = 0.0$  Å) for the cis simulations (vestibule → periplasmic), and at  $z = -12$  Å from the constriction region for the trans simulation (periplasmic → vestibule) in monomer OmpF (see Figure 1). Initial relaxation of the system with the ampicillin was performed for 2 ns at constant volume and temperature using the MD software package ORAC.<sup>20</sup>

The process of ampicillin translocation occurs on a timescale ( $\sim 200 \mu\text{s}$ )<sup>21</sup> which cannot be reached by standard MD simulations with an all-atom representation. To overcome this problem we used the metadynamics algorithm.<sup>10</sup> This algorithm, based

on a history dependent biasing potential added in a subspace defined by a chosen set of reaction coordinates  $s_a(x)$  is aimed at reconstructing the multidimensional free energy of a given process. At time  $t$  the biasing potential  $V_G$  is given as the sum of repulsive Gaussian functions added with a frequency  $1/\tau_G$

$$V_G(s(x), t) = W \sum_{\substack{t'=\tau_G, 2\tau_G, 3\tau_G, \dots \\ t' < t}} \exp\left(-\frac{(s(x) - s_G(t'))^2}{2(\delta s)^2}\right) \quad (1)$$

where  $W$  is the Gaussian height,  $\delta s$  is the Gaussian width. Due to this potential, the system is discouraged from revisiting the configurations already sampled. Metadynamics, not only allows the acceleration of rare events, but also the reconstruction of the free energy  $F_G(s, t) = -V_G$ , which is an approximation of  $F(s)$  in the region  $\Sigma(s)$  explored by  $s(x_{G(t)})$  up to time  $t$ .<sup>22</sup> The accuracy of free energy reconstruction is dependent upon the Gaussian parameters  $W$ ,  $\delta s$  and  $\tau_G$ . Details of the metadynamics algorithm have been previously described.<sup>10,22,23</sup>

**Choice of Reaction Coordinates.** The choice of reaction coordinates is pivotal to obtain the best approximation of the free energy. As suggested in previous studies, the orientation of ampicillin<sup>24</sup> together with the matching of its dipole with the transversal electric field<sup>11,12</sup> is crucial for its binding at the constriction region. The long axis of ampicillin is also the largest component of its electric dipole. Therefore, we decided to introduce an explicit coordinate to improve the description of the diffusion process. The two reaction coordinates (RCs) chosen to accelerate the passage of ampicillin through OmpF are (i) the distance  $Z$  defined as the difference between the antibiotic's center of mass and the system's (porin + detergent) center of mass along the  $z$  axis and (ii) the angle  $\theta$  defined as the dot product between the long axis of the molecule and the  $z$  axis of OmpF. The Gaussian parameters chosen are  $\tau_G = 4$  ps,  $W = 0.24$  kcal/mol, and  $\delta s = 0.3$  Å for the distance  $Z$  and  $\delta s = 5.0^\circ$  for the angle, selected to allow a better resolution in the sampling of the free energy and a low error value (up to 2 kcal/mol).<sup>22</sup>

Here, we used metadynamics as an exploratory method to identify the different minima along the channel. Then, we performed additional metadynamics simulations to calculate the free energy barriers connecting all of the minima. The “forward” energy barriers connecting each minimum (for example from Mini-I to Mini-II) was evaluated by counting the contour lines separating each minimum from “top to bottom” in the free energy surface (FES) resulting from the translocation simulation. To obtain the “backward” energy barriers connecting each minimum (for example from Mini-II to Mini-I), we launched additional metadynamics simulations starting from each minimum identified and simulated the reverse process. From this new FES obtained, we then evaluated the “backward” energy barriers by counting the lines separating each minimum from “bottom to top”. In the end we put together the “forward and backward” energy barriers in the 1D free energy profile (1D-FEP) that thus sums up the complete energetic of the translocation process. From the 1D-FEP we can evaluate the effective barrier of translocation  $\Delta G$  as the difference between the energy at highest barrier and at the entrance of the antibiotic in the channel.

From each identified minimum we performed additional standard MD simulations (up to 4 ns) to characterize the structural details and the interaction of ampicillin with OmpF. The hydrogen bonds (Hbond) between OmpF and ampicillin

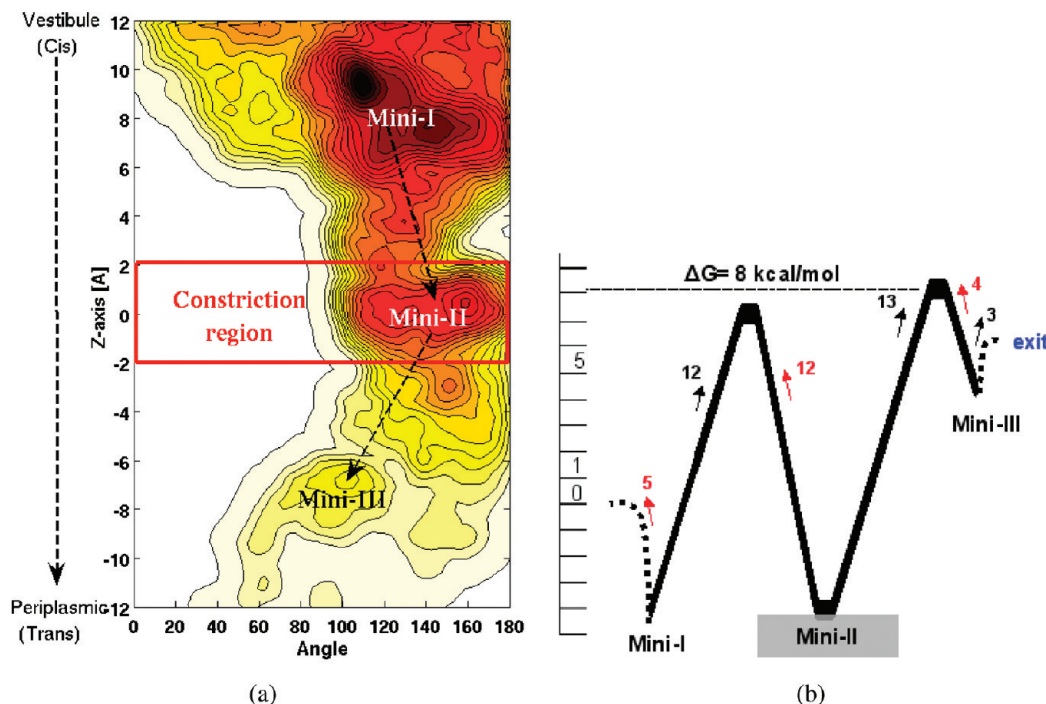


**Figure 2.** Free energy surface and 1-dimensional profile. In panel a, two-dimensional free energy surface of ampicillin's translocation process (cis → trans). Each color corresponds to energy difference 1 kcal/mol. In panel b, we show, 1-dimensional free energy profile for ampicillin translocation through OmpF.

are counted using VMD<sup>25</sup> scripts with the following threshold parameters: a distance of at most 2.8 Å and donor–hydrogen–acceptor angle of at least 130°. Hydrophobic contacts (Hphobic) are counted when nonpolar atoms are separated by at most 3 Å. We define durable Hbonds as the ones that have a lifetime equal to or higher than 20% of simulation time.

The change in enthalpy energy of ampicillin in the different minima identified was done by evaluating the nonbonded interactions (van der Waals + electrostatics) between ampicillin and all other atoms (protein, ions, water molecules) which lie within a cutoff of 10.0 Å from ampicillin, and for electrostatic interactions we adopt the same scheme (soft particle mesh Ewald schemes<sup>26</sup>) as for the simulations. The configurational entropy of ampicillin in the different minima was calculated from the covariance matrices of the atomic fluctuations as proposed by Andricioaei and Karplus.<sup>27</sup>

Further, these standard MD simulations were used to evaluate interactions between the water molecules and ampicillin at each minimum. The survival probability for the water molecules in three different time regimes (fast, medium, slow) bound to ampicillin was calculated as mentioned in Sterpone et al.<sup>28</sup> We then used the following function:

$$F(t) = n_{\text{fast}} \exp\left[-\left(\frac{t}{\tau_{\text{fast}}}\right)^c\right] + n_{\text{medium}} \exp\left[-\left(\frac{t}{\tau_{\text{medium}}}\right)\right] + n_{\text{slow}} \exp\left[-\left(\frac{t}{\tau_{\text{slow}}}\right)\right] \quad (2)$$

to fit the survival probability and extract the different temporal scales and the associated number of water molecules. In eq 2, the first term corresponds to the fast regime (around 15 ps), the second, to the medium regime (around 100 ps), and the last term, to the slow regime (greater than 100 ps). The variables  $\tau_{\text{fast}}$ ,  $\tau_{\text{medium}}$ , and  $\tau_{\text{slow}}$  are the different relaxation times, and  $n_{\text{fast}}$ ,

$n_{\text{medium}}$ , and  $n_{\text{slow}}$  correspond to the average number of water molecules in the three different regimes.

## Results

**Energetic Details of the Translocation of Ampicillin through OmpF.** Ampicillin translocates through OmpF-WT, from the vestibule to the periplasmic space, in a biased simulation time of ~38 ns, populating (deep) minima in free energies that can be related to well-defined locations inside the channel, see Figure 2a. These minima are located above the constriction region (Mini-I), at the constriction region (Mini-II), and also below the constriction region (Mini-III) as shown in Figure 2a. Above the constriction region the polar oxygens of ampicillin are involved in transient Hbond interactions with basic residues R167, R168, and K80. As ampicillin slides down to reach and cross the constriction region, there is always a Hbond between its carboxylic group and one of the positively charged residues on the anti-L3 side of the constriction region. To support this observation, in Figure 4, we show the minimal distance, throughout the simulation time, between the (hydrogen bond acceptors) two oxygens (O, OXT; see Figure 3) of the ampicillin and either of the (hydrogen bond donors) residues present in the anti-L3 side: R132, R82, R42, and K16. This allows us to distinguish ampicillin in the central part of the channel (where the distance remains ~3 Å) from the regions where ampicillin reorients above and below the constriction region (where the distance fluctuates ~10 Å). We then calculated the energy barriers connecting each minimum along the translocation path (see Materials and Methods) and reconstructed the 1D free energy profile, shown in Figure 2b. The profile shows that ampicillin has to overcome two large free energy barriers to translocate: (i) a barrier of 12 kcal/mol to go from Mini-I to Mini-II and (ii) a barrier of 13 kcal/mol to go from Mini-II to Mini-III. The energy landscape obtained from metadynamics simulations reveals that ampicillin follows the 2B-1BS model when translocating through OmpF.<sup>13,29</sup> The

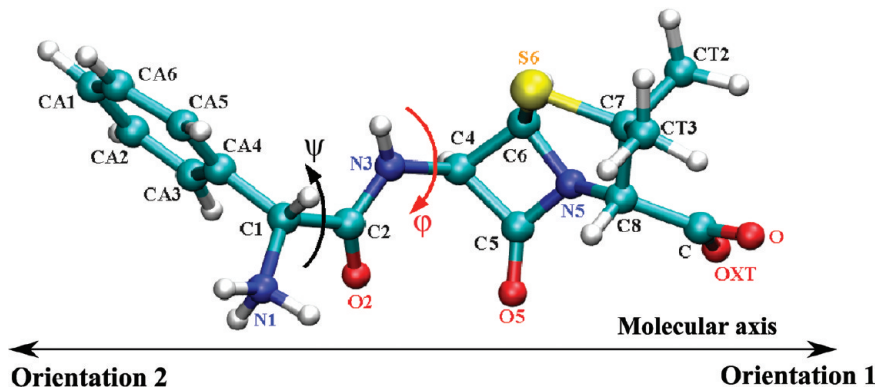


**Figure 3.** Ampicillin (Amp) is shown using ball and stick representation. Oxygen atoms in red, nitrogen atoms in blue, carbon atoms in cyan, sulfur atom in yellow, and hydrogen atoms in white. The atoms forming ramachandran torsions ( $\phi$ ,  $\psi$ ) are:  $\phi$  torsion W1: C2–N3–C4–C5;  $\psi$  torsion W2: CA4–C1–C2–N3.

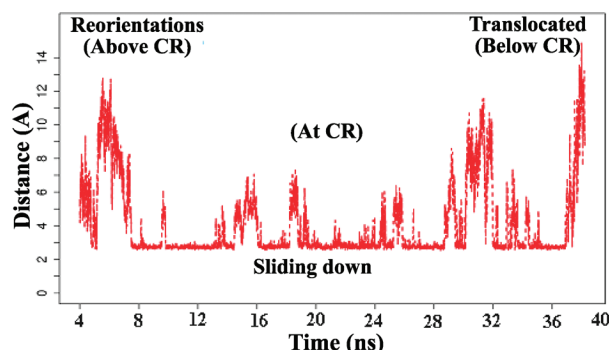


**Figure 4.** Plot of the minimum distance between carboxy group ( $\text{COO}^-$ ) of ampicillin and any positive group of the basic residues (R132, R82, R42, and K16) along metadynamics simulations is shown here.

calculated main energy barrier  $\Delta G$  is 8.0 kcal/mol, in good agreement with the one estimated from recent electrophysiology experiments ( $13 k_B T \sim 7.8$  kcal/mol).<sup>30</sup>

**Molecular Details of Ampicillin's Translocation from Equilibrium Simulations.** We performed additional MD simulations to analyze dynamical and structural properties of ampicillin in the three minima identified along the translocation path. In the first minimum, above the constriction region (mini-I), ampicillin undergoes many reorientations in relation to the numerous attempts to accommodate into the constriction region. This would imply a high entropic barrier to go from Mini-I to Mini-II. The image displayed in Figure 5a highlights the different conformations of the antibiotic as it makes only transient interactions with partners in OmpF which are diversely located above or at the constriction region of OmpF (R167, R168, S125, R132, Q66, M38, and F118). In Mini-I, we measure a total of 14 Hbonds between ampicillin and diverse residues of OmpF, of which only 3 Hbonds are durable (i.e., having a lifetime  $\geq 20\%$  of simulation time). The important flexibility of ampicillin in mini-I is further evident from ampicillin's large average root-mean-square fluctuations (rmsf) of 0.78 Å and in the large value of configurational entropy calculated to be  $TS = 7.2$  kcal/mol. We also find broad distribution for the angle  $\theta$  (the second reaction coordinate), highlighting also a large orientational entropy of ampicillin in Mini-I (see Table 1A or Figure S2 in Supporting Information). Interestingly, simulating ampicillin in bulk water we find quite similar fluctuations (rmsf  $\sim 1.0$  Å,  $TS = 8.5$  kcal/mol) and distribution for its angle  $\theta$  (data not shown). Once ampicillin positions itself vertically with its carboxylic group pointing downward (see orientation 1 in Figure 3), it quickly diffuses toward the CR, where it enters

Mini-II. Along the standard MD simulations at Mini-II, we find a lower value for ampicillin's fluctuation (rmsf  $\sim 0.29$  Å, see Table 1A) and a decrease ( $TS = 5.3$  kcal/mol) in the configurational entropy of ampicillin, with respect to Mini-I. This is expected, considering the narrow pore size at the CR which limits the allowed conformations of ampicillin, also evident from a narrow distribution for angle  $\theta$  (see Table 1B), which highlights the decrease in the orientational entropy of ampicillin. This loss in entropy (both configurational and orientational) with respect to mini-I is compensated by a gain in enthalpy ( $\Delta H \sim 24$  kcal/mol, of which 20 kcal/mol is from the electrostatics and 4 kcal/mol is from the van der Walls, see Table 1B). Indeed ampicillin develops a favorable network of interactions with residues at the pore, 6 durable Hbonds measured (see Table 1B). In particular, see Figure 5b, ampicillin is stabilized by strong Hbonds: one between its N-terminal positive group (amino group) and D113 on the L3-side and the others, on the anti L3-side, between its oxygens and the basic residues R132, R82, R42, and K16. Additionally, the phenyl and the dimethyl (CT2 and CT3) groups of ampicillin also make important Hphobic interactions with partners on the L3-side (F118, P116, and L115) of OmpF. Finally, as ampicillin moves from Mini-II to Mini-III, we find important interactions between ampicillin and OmpF, in particular Hbond interactions between the positively charged N-terminal group and residue D113 (see Figure 5c). Interestingly, in Mini-III, which lies below the constriction region, we recover the large fluctuations of ampicillin (0.40 Å, see Table 1A) and estimated an increase in the configurational entropy of ampicillin ( $TS = 6.2$  kcal/mol) with respect to Mini-II.

**Role of Solvation.** OmpF is classified as a water-filled pore.<sup>31–33</sup> Previous studies<sup>8,9</sup> have shown the ordering of water molecules at the constriction region due to the presence of the high transversal electric field. Here, we went further and analyzed the number and the residence time of water molecules interacting with the translocating antibiotic in each identified minimum (see Table 1A). Interestingly, the average number of interacting water molecules is stable along all three minima and is of around 20, confirming the water-filled character of OmpF channel. Instead, the differences between the three minima can be seen in the residence time of water molecules interacting with ampicillin. As expected, when ampicillin is placed in a box of water, the residence time of all water molecules interacting with ampicillin does not exceed 15 ps, revealing an exclusively quick exchange with the outer shell. The presence of water molecules in such a fast regime is also high in all three minima, respectively 82%, 63%, and 96%. However, it is only in

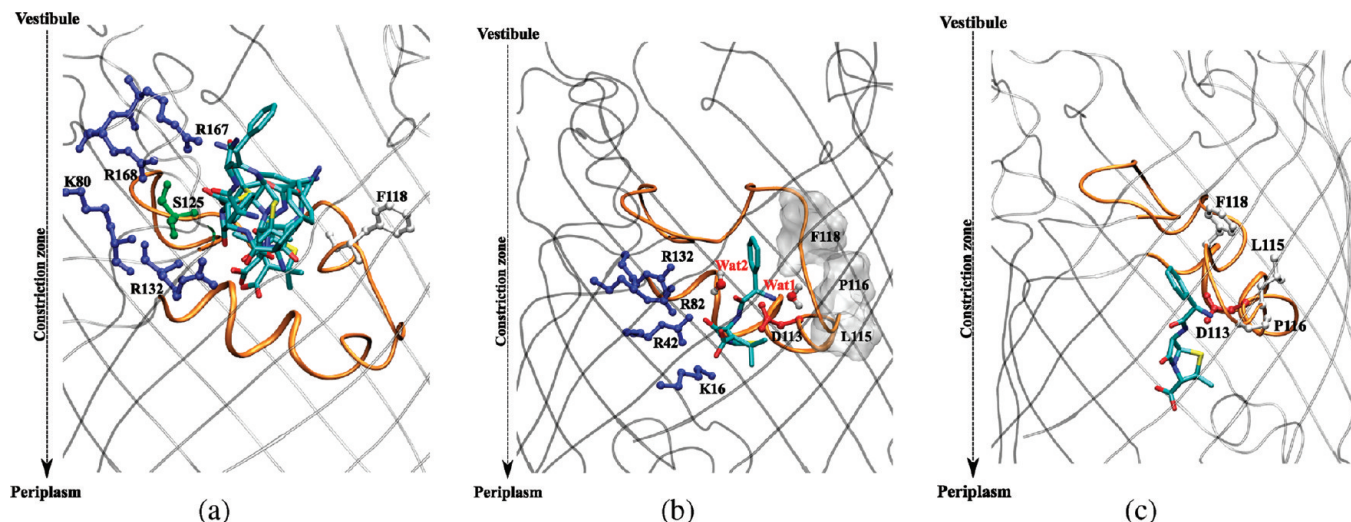


**Figure 5.** Three steps depicting the mechanism of ampicillin's (Amp) translocation through OmpF. Only the residues involved in Hbond/Hphobic interactions with ampicillin are shown here. The residues of OmpF monomer are represented using ball-sticks representation (basic: blue, acidic: red, hydrophobic: gray), and the H-phobic pockets are shown in surf representation (gray). In panel a, numerous orientation of ampicillin above the CR is shown corresponding to step 1. In panel b, diverse interactions at the CR (mini-II) and two persistent water molecules involved in salt-bridging interactions is shown. In panel c, the concluding interaction between OmpF and Amp before translocation is shown (step 3).

**TABLE 1: In Depth Analysis of Ampicillin's Solvation and Fluctuation in Water Box and along Each Minima from Standard MD Simulations<sup>a</sup>**

A. Solvation and Fluctuation of Ampicillin						
trajectory	average number	water analysis				
		fast (%)	medium (%)	slow (%)	RMSF (Å)	
water box	31.0	100	0	0	0.99	
mini I	21.5	82	18	0	0.74	
mini II	23	63	27	10	0.29	
mini III	22.5	96	0	4	0.40	

B. Entropy and Enthalpy Change of Ampicillin						
trajectory	Hbonds		angle $\theta$ distribution	$T\Delta S$ , kcal/mol	$\Delta H$ (kcal/mol)	
	transient	durable			VdW	electrostatic
mini I	11	3	[80:120]	2.0	4.2	20.0
mini II	3	6	[125:145]	0.0	0	0
mini III	2	1	[70:105]	1.0	10.0	18.7
C. Population States for Torsions W1 and W2						
trajectory	P(W1) in %			P(W2) in %		
	A [-200:-140]	B [-110:-40]	C [-10:30]	D [-100:-30]	E [50:180]	End to end distance (Å)
water box	46	52	2	22	70	$8.6 \pm 0.3$
mini I	0	64	25	0	98	$8.0 \pm 0.3$
mini II	0	0	100	0	98	$7.0 \pm 0.3$
mini III	0	100	0	96	0	$8.2 \pm 0.2$

<sup>a</sup> In part A, the first four columns show the number and percentage of waters molecules in different time regimes. In the last column the average fluctuation of ampicillin is shown. In part B, the first two columns represent the transient and durable Hbonds, the third column for the orientational entropy: probability distribution for angle  $\theta$  (the second reaction coordinate) in the three minima is reported. In the fourth column the change in configurational entropy energy of ampicillin is reported. In the next two columns, enthalpy energy decomposed into van der Waals (VDW) and electrostatics and in the last column the total change in enthalpy energy of ampicillin in the three minima are reported. In part C, the first three columns represent the populated states of torsion W1 and last two columns represent the population states of torsion W2 (in %), and the end-to-end distance highlighting the compactness of ampicillin is represented in last column.

mini-II that the water exchange significantly slows down, reflected by the 27% medium and 10% of slow waters. In particular, the latter corresponds to two water molecules (Wat1 and Wat2) bridging ampicillin and OmpF on both sides of the constriction region. As seen in Figure 6, Wat1 bridges ampicillin (N1) with F118 (O) and L115 (O), whereas Wat2 bridges ampicillin (O2) and ampicillin (O5) with R132 (NH). We expect that the interactions of ampicillin with the slow water molecules will constitute an additional enthalpic term favoring the binding at the constriction

region. We also performed additional MD simulation of the pore (in Mini-II) in the absence of ampicillin. Interestingly, we find the two slow water molecules to be present at the constriction region. Therefore, we believe that there is a little contribution to the entropic change of these water molecules on the overall change in the free energy in the mechanism.

**Role of Internal Coordinates (Torsion Angles W1 and W2).** In our previous study,<sup>11</sup> we noted the importance of the internal degrees of freedom, i.e., torsion angles W1 and W2 of

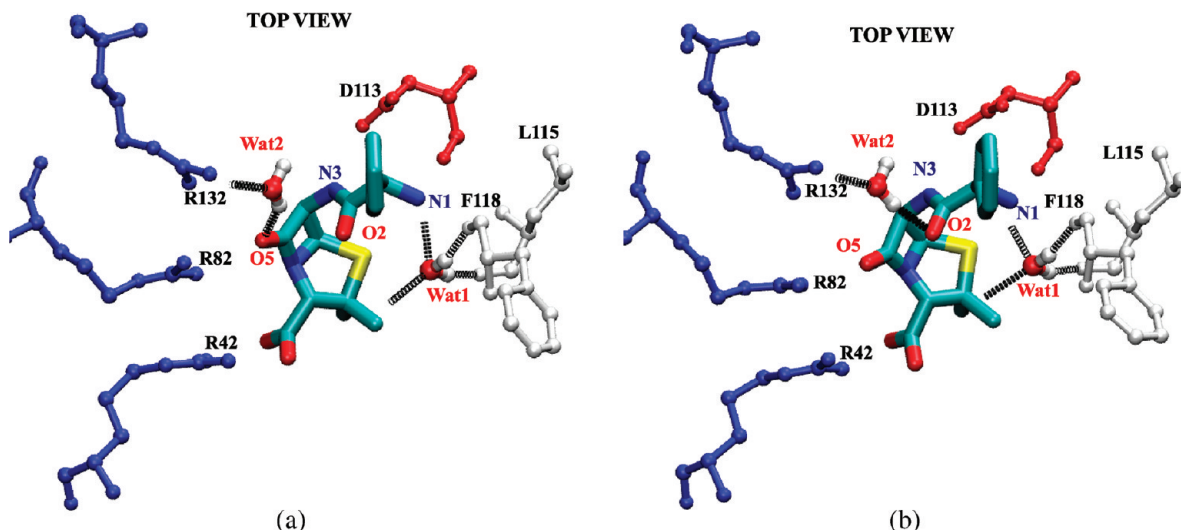


**Figure 6.** Water mediated salt bridge and stabilizing interaction between OmpF and Amp is shown here. The Hbond interactions between water molecules with either OmpF or Amp is shown in solid black lines. In panel a, the salt-bridge interaction involving O5 atom of Amp with OmpF is shown, and in panel b, the salt-bridge interaction involving O2 atom of Amp with OmpF is shown.

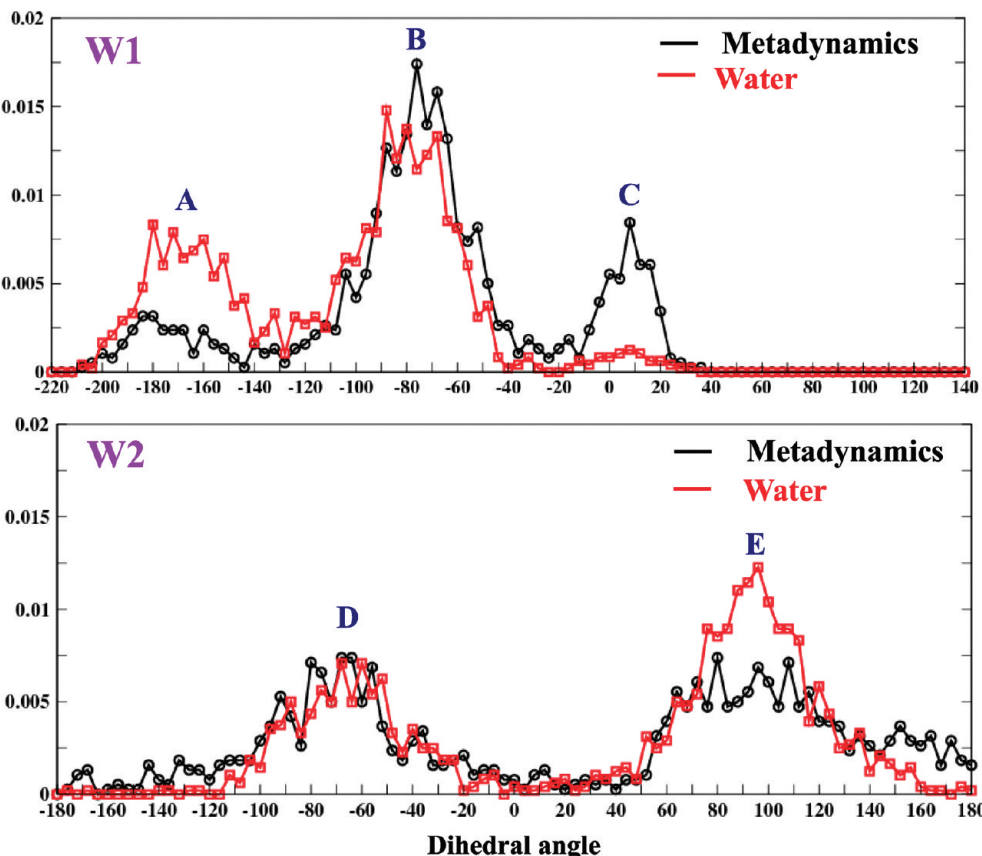


**Figure 7.** Possible population states for torsions W1 and W2. We see three states of W1: A [-200:-140], B [-110:-40], and C[-10:30] and two states of W2: D [-110:30] and E [50:180] degrees.

ampicillin (see Figure 3 for their atomic definition), during the passage through the CR. Here, we went further by analyzing the distributions of W1 and W2 along the complete translocation process. In Figure 7, we show the W1/W2 distribution for different simulations; (i) when ampicillin is in a box of water, (ii) during its complete translocation through OmpF, and (iii) when placed on each minimum identified (see Table 1B). We find that state C of W1 occurs predominantly at the CR (Mini-II). Moreover, this state corresponds to a more compact form of ampicillin, which is highlighted by the short end-to-end distance calculated between the atoms N1 and C (see Figure 3

for labels),  $7.0 \pm 0.3 \text{ \AA}$ . However, in mini-I and mini-III this distance is  $8.0 \pm 0.3 \text{ \AA}$  (see Table 1C). On the other hand, state E of torsion angle W2 is not only present at the CR (Mini-II), but also above CR (Mini-I) as well as in bulk water. This suggests that one of the main rate-limiting step for translocation of ampicillin through OmpF is the transition to state C for angle W1.

To test this hypothesis, we repeated simulations where torsion angle W1 of ampicillin is constrained alternatively to (i) the favorable state C and (ii) the unfavorable state B, by applying a harmonic force constant of 24 kcal/mol. The analysis of the

**TABLE 2: Changes at the Constriction Region, on Constraining W1 to the Favorable and Unfavorable Values**

parameters	W1 torsion	
	constrained to C	constrained to B
population of other torsion end to end distance (Amp)	no changes of W2 was observed $6.5 \pm 0.3 \text{ \AA}$	W2 changes to state D (instead of E) $8.5 \pm 0.2 \text{ \AA}$
main barrier translocation	3.8 kcal/mol	9.0 kcal/mol

constrained simulations is summarized in Table 2. We note that when W1 is constrained to its favorable state C, the torsion angle W2 also maintains its favorable state B and the end-to-end distance of ampicillin decreases by  $\sim 0.5 \text{ \AA}$  compared to the unconstrained simulation (see Table 1). The presence of favorable states for both the torsion angles W1 and W2 and the compact conformation of ampicillin yield to give a lower effective energy barrier of translocation (3.8 kcal/mol; see Table 2 or Figure S1 in the Supporting Information for the 1D-FES profile). Thus, this suggests that preorganizing ampicillin in an optimal conformation for the constriction region would increase its flux through OmpF. Instead, when constraining W1 to its unfavorable state B, we find drastic changes in the states visited by the torsion angle W2 along the channel. As a consequence, ampicillin stays longer above the constriction region. In this case, we observe strong Hbond interactions between the amino group (N1 atom of Amp) and E117, which constitutes a clear difference with respect to the unconstrained simulations yielding a slight increase (by  $\sim 1 \text{ kcal/mol}$ ) in the effective barrier of translocation. This small difference in energy is probably due to the fact that when we constrain W1 to its unfavorable state B, this is also the most populated state above CR as well as in bulk water. On the other hand, the high gain ( $4 \text{ kcal/mol}$ ) in the main barrier obtained in preorganizing W1 to C is not only due a decreased entropic barrier. From the simulation of ampicillin in water-box, the evaluated entropic barrier for torsion angle W1 to arrive to state C is 2.5 kcal/mol, thus the remaining difference is part of the enthalpic contribution upon preorganization. As suggested by a previous study,<sup>34</sup> the energetic consequences upon preorganization are a combination of both entropic and enthalpic components, such as the more compact form adopted by ampicillin that can favor different interactions.

**Inverse Translocation Process of Ampicillin through OmpF.** In electrophysiology experiments, OmpF is reconstituted into an artificial planar lipid bilayer, and on addition of ampicillin, fluctuations in ion current occur, allowing the kinetics of binding to be quantified.<sup>14</sup> Then, by means of the two-barrier-one-binding-site model, the flux is estimated.<sup>35</sup> The reliability of this model is based on the unicity of the binding site, verified by the identical distribution of residence times upon addition of antibiotic on the cis and trans side.<sup>14</sup> However, this identity is not a direct proof of the unicity of the binding site, as we have recently demonstrated using molecular simulations of another antibiotic (enrofloxacin) for which we find two symmetric binding sites located at both mouths (cis/trans) channel.<sup>36</sup>

To address the existence of the unique affinity site, we performed an additional metadynamics simulation placing ampicillin at the periplasmic (trans) side in order to investigate the inverse translocation process (periplasm  $\rightarrow$  vestibule). The free-energy landscape presented in Figure 8a reveals the existence of a deep affinity site at constriction region (Mini-II'), which has the same localization as Mini-II, that was reached

placing ampicillin in the vestibule end. To characterize the structure and dynamics of ampicillin in this affinity site (mini-II'), we performed an additional equilibrium simulations. As seen from Figure 8b, here we find ampicillin to be also oriented in a similar way as in Mini-II with its carboxy group pointing downward (see Figure 8b). In Mini-II' ampicillin is involved in Hbond and Hphobic contacts and interaction with water molecules in a similar way as in Mini-II, further supported by nearly identical value for enthalpy term in Mini-II', i.e.,  $-249 \text{ kcal/mol}$  compared to  $-248.6 \text{ kcal/mol}$  in Mini-II. Further, the analysis of the torsion angles at the constriction region revealed that, exactly as in Mini-II, W1 and W2 are populated with state C and state E respectively. As a whole, we prove the microscopic unicity of the affinity site for ampicillin in OmpF, accessible from both side of the channel, thus confirming experimental findings.<sup>14</sup>

## Discussion and Conclusions

Here we propose a multiscale approach (i) first using metadynamics as a coarse grained method to explore the free energy surface of the translocation process and (ii) then performing additional simulations on each minimum to evaluate the energetics and interaction network between OmpF and ampicillin. From our detailed analysis, we can identify the structural determinants for ampicillin translocation through OmpF.

The translocation process of ampicillin through OmpF fits well into the 2B-IBS model previously proposed to quantify the flux of sugar molecules through specific channels such as the bacterial porin LamB.<sup>13</sup> From our study, we find a unique affinity site at the constriction region for ampicillin, accessible from both sides of the channel, in accordance with electrophysiology experiments.<sup>14,30</sup> This main affinity site is microscopically characterized by specific interactions, a well-defined orientation (see orientation 1; Figure 3) and unique values for the torsion angles W1 and W2. Ampicillin reaches the CR by taking advantage of the entropy/enthalpy compensation. In particular, we identified the Hbonded, Hphobic and water mediated interactions between ampicillin and OmpF which strengthen the enthalpic contribution ( $\Delta H = 24 \text{ kcal/mol}$ , where  $20 \text{ kcal/mol}$  are from the electrostatics and  $4 \text{ kcal/mol}$  from the van der Walls), compensating the loss in entropy in mini-II ( $T\Delta S \sim 2 \text{ kcal/mol}$ ). Our findings point toward a correct trend for the entropy-enthalpy compensation in permeation of antibiotic through the channel. The enthalpy gain,  $24 \text{ kcal/mol}$ , is found to correlate with the important network of interactions at the constriction region, and we expect that this is compensated by the sum of all entropic terms accounting for the differences between the ampicillin above and at the constriction region. The difference between the calculated enthalpy and entropy is due to missing contributions: (i) the enthalpy of protein–water molecules when the latter move from Mini-II to Mini-I for the displacements of ampicillin and (ii) other entropy terms such as the contribution from the protein and water molecules upon movement of ampicillin.

We propose that there should be an optimal ampicillin-ompf association at the constriction region to facilitate the antibiotic permeation process, avoiding strong binding that would lead to saturation, also discussed in previous studies.<sup>29,37</sup> Interestingly, this optimization is done thanks to similar contributions as in enzymes, discussed by Warshel and co-workers:<sup>38</sup> (i) electrostatic preorganization and steric strains at the constriction region, (ii) solvation, (iii) entropy, and (iv) enthalpy changes of the ampicillin. Furthermore, we found that torsion angle W1 has a

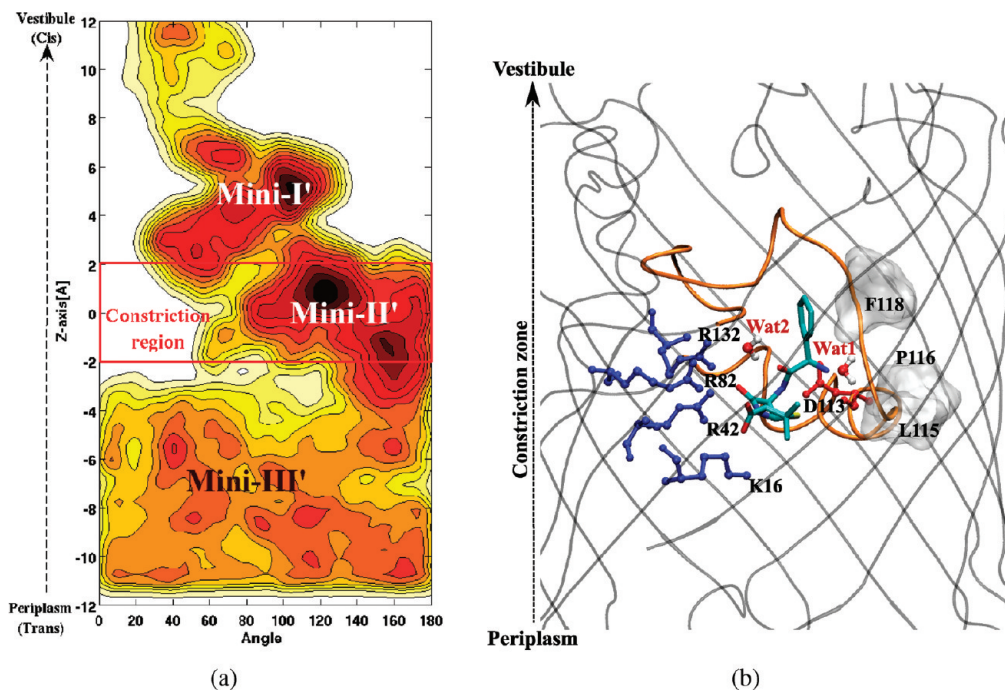


**Figure 8.** Inverse Translocation of ampicillin through OmpF. In panel a, two-dimensional free energy surface for the translocation process is shown. In panel b, we show the conserved affinity site at the CR for the translocation process.

preferential value at the constriction region, corresponding to a compact form of ampicillin. The transition to this compact form is one of the main rate-limiting step for ampicillin's translocation. Indeed, we showed that by preorganizing ampicillin in the optimal conformation for the binding at the constriction region, the energy barrier of translocation is lowered by 4 kcal/mol. A similar approach has been exploited in enzyme-ligand studies to optimize the interactions by preorganizing the ligand, thus lowering the entropic barrier of the complex formation.<sup>39</sup>

On the porin side we note the presence of the basic residues oriented as a staircase (R167, R168, K80, R132, R82, R42, and K16 from vestibule to periplasmic) along one side of the channel (see Figure 9) which provides favorable interactions between the polar oxygen atoms of ampicillin and facilitates its translocation. This finding is in agreement with a similar arginine ladder that was shown to facilitate phosphate transfer<sup>40</sup> in the OM protein OprP as well as the greasy slide found in maltoporins.<sup>41</sup> The presence of highly ordered water molecules at the constriction region and the fact that they are involved in multiple hydrogen bonds with high residence time might explain the difficulty in the diffusion of hydrophobic molecules across OmpF.<sup>4</sup> Furthermore, the localization of hydrophobic pockets above the constriction region (M38 and F118) and behind the L3 loop (M114, L115, and P116), is seen to play an important role in the translocation of ampicillin across OmpF (see Figure 9). The position of two functional groups of ampicillin, the phenyl ring and dimethyl groups (CT2 and CT3; see Figure 3) allows ampicillin to fit well into these hydrophobic pockets.

To sum up, in the current study, we have presented a complete analysis of the translocation of an antibiotic through the bacterial porin OmpF, providing insight into the key determinants for the uptake process. These are the specific interactions at the constriction region, the internal degrees of freedom and the interaction with the solvent. Having identified the key/specific interactions between the pore-antibiotic, and now having decomposed the energetics into enthalpy and entropy components, the next step will be to use this information to predict modification in antibiotic which would allow it to translocate

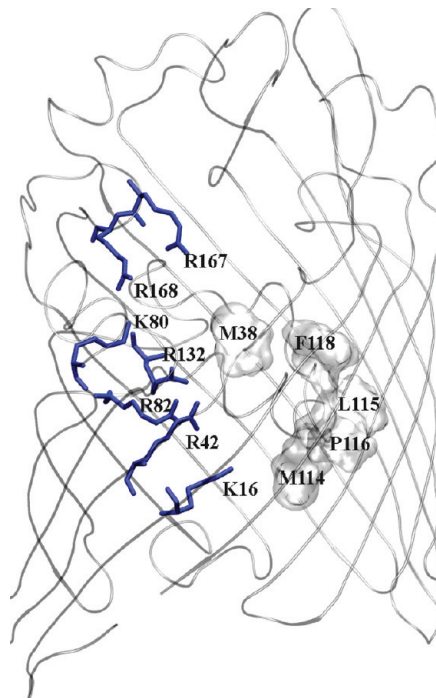


**Figure 9.** Key determinants in OmpF which facilitate Amp translocation. The staircase of basic residues are in blue and hydrophobic pockets in white.

faster by interacting differently with the pore. Here, we used ampicillin and OmpF as a test case even though we believe that such analysis can be extended to other classes of antibiotics and porins. A major current dilemma for the pharmaceutical industry is whether to develop new drugs or promote those presently on the market.<sup>42</sup> In this scenario, the information (preorganization, solvation, entropy/enthalpy compensations) gathered from our simulations could be used as an input toward designing antibiotics with optimal physicochemical properties, allowing them to translocate with a higher rate through porins.

**Acknowledgment.** This study was supported by EU Grant MRTN-CT-2005-019335 (Translocation). The authors thank CPU hours provided by Cybersesar (Cagliari), Caspur (Rome), and Cineca (Bologna). We also thank Prof. Malcolm Page and Dr. Juerg Dreier (Basilea Pharmaceutica) for useful discussions. A.K. thanks Dr. P. L. Palla (University of Cagliari) for technical support.

**Supporting Information Available:** Figure S1: 1-Dimensional free energy profile of ampicillin translocation with torsion angle W1 fixed to state C. Figure S2: Angle  $\theta$  (second reaction coordinate) distribution plot for standard MD simulations in the minima. This material is available free of charge via the Internet at <http://pubs.acs.org>.

## References and Notes

- (1) Cars, O.; Hogberg, L. D.; Murray, M.; Nordberg, O.; Sivaraman, S.; Lundborg, C. S.; So, A. D.; Tomson, G. *Brit. Med. J.* **2008**, *337*, 726.
- (2) Cowan, S. W.; Schirmer, T.; Rummel, G.; Steiert, M.; Ghosh, R.; Pauput, R. A.; Jansonius, J. N.; Rosenbusch, J. P. *Nature* **1992**, *358*, 727.
- (3) Yamashita, E.; Zhalnina, M. V.; Zakharov, S. D.; Sharma, O.; Cramer, W. A. *EMBO J.* **2008**, *27*, 2171.
- (4) Nikaido, H.; Rosenberg, E. Y. *J. Bacteriol.* **1983**, *153*, 241.
- (5) Schulz, G. E. *BBA-Biomembr.* **2002**, *1565*, 308.
- (6) Schulz, G. E. *Curr. Opin. Cell. Biol.* **1993**, *5*, 701.
- (7) Nikaido, H. *Microbiol. Mol. Biol. Rev.* **2003**, *67*, 593.
- (8) Im, W.; Roux, B. *J. Mol. Biol.* **2002**, *319*, 1177.
- (9) Robertson, K. M.; Tielemans, D. P. *FEBS Lett.* **2002**, *528*, 53.
- (10) Laio, A.; Parrinello, M. *Proc. Natl. Acad. Sci. U.S.A.* **2002**, *99*, 12562.
- (11) Ceccarelli, M.; Danelon, C.; Laio, A.; Parrinello, M. *Biophys. J.* **2004**, *87*, 58.
- (12) Danelon, C.; Nestorovich, E. M.; Winterhalter, M.; Ceccarelli, M.; Bezrukova, S. M. *Biophys. J.* **2006**, *90*, 1617.
- (13) Benz, R.; Schmid, A.; Vos-Scheperkeuter, G. *J. Membr. Biol.* **1987**, *100*, 21.
- (14) Nestorovich, E. M.; Danelon, C.; Winterhalter, M.; Bezrukova, S. M. *Proc. Natl. Acad. Sci. U.S.A.* **2002**, *99*, 9789.
- (15) Jusuf, S.; Loll, P. J.; Axelsen, P. H. *J. Am. Chem. Soc.* **2002**, *124*, 3490.
- (16) Duntiz, J. D. *Chem. Biol.* **1995**, *2*, 709.
- (17) Rostovtseva, T. K.; Nestorovich, E. M.; Bezrukova, S. M. *Biophys. J.* **2002**, *82*, 160.
- (18) Cornell, W. D.; Cieplak, P.; Bayly, C. I.; Gould, I. R.; Merz, K. M.; Ferguson, D. M.; Spellmeyer, D. C.; Fox, T.; Caldwell, J. W.; Kollman, P. A. *J. Am. Chem. Soc.* **1995**, *117*, 5179.
- (19) Ceccarelli, M.; Marchi, M. *J. Phys. Chem. B* **2003**, *107*, 1423.
- (20) Procacci, P.; Darden, T. A.; Paci, E.; Marchi, M. *J. Comput. Chem.* **1997**, *18*, 1848.
- (21) Hajjar, E.; Mahendran, K. R.; Kumar, A.; Bessonov, A.; Petrescu, M.; Weingart, H.; Ruggerone, P.; Winterhalter, M.; Ceccarelli, M. *Biophys. J.* **2010**, *98*, 569.
- (22) Laio, A.; Rodriguez-Fortea, A.; Gervasio, F. L.; Ceccarelli, M.; Parrinello, M. *J. Phys. Chem. B* **2005**, *109*, 6714.
- (23) Laio, A.; Gervasio, F. L. *Rep. Prog. Phys.* **2008**, *71*, 1.
- (24) Vidal, S.; Bredin, J.; Pages, J.-M.; Barbe, J. *J. Med. Chem.* **2005**, *48*, 1395.
- (25) Humphrey, W.; Dalke, A.; Schulten, K. *J. Mol. Graphics* **1996**, *14*, 33.
- (26) Essmann, U.; Perera, L.; Berkowitz, M. L.; Darden, T.; Lee, H.; Pedersen, L. G. *J. Chem. Phys.* **1995**, *103*, 8577.
- (27) Andricioaei, I.; Karplus, M. *J. Chem. Phys.* **2001**, *115*, 6289.
- (28) Sterpone, F.; Ceccarelli, M.; Marchi, M. *J. Mol. Biol.* **2001**, *311*, 409.
- (29) Berezhkovskii, A. M.; Bezrukova, S. M. *Biophys. J.* **2005**, *88*, L17.
- (30) Mahendran, K.; Chimerel, C.; Mach, T.; Winterhalter, M. *Eur. Biophys. J.* **2009**, *38*, 1141.
- (31) Benz, R.; Schmid, A.; Vos-Scheperkeuter, G. *Eur. J. Biochem.* **1988**, *176*, 1.
- (32) Buehler, L. K.; Kusumoto, S.; Zhang, H.; Rosenbusch, J. P. *J. Biol. Chem.* **1991**, *266*, 24446.
- (33) Nikaido, H. *J. Biol. Chem.* **1994**, *269*, 3905.
- (34) Benfield, A. P.; Teresk, M. G.; Plake, H. R.; DeLorbe, J. E.; Millspaugh, L. E.; Martin, S. F. *Angew. Chem., Int. Ed.* **2006**, *45*, 6830.
- (35) Schwarz, G.; Danelon, C.; Winterhalter, M. *Biophys. J.* **2003**, *84*, 2990.
- (36) Mahendran, K. R.; Hajjar, E.; Mach, T.; Lovelle, M.; Kumar, A.; Sousa, I.; Spiga, E.; Weingart, H.; Gameiro, P.; Winterhalter, M.; Ceccarelli, M. *J. Phys. Chem B* **2010**, *114*, 5170.
- (37) Bauer, W. R.; Nadler, W. *Proc. Natl. Acad. Sci. U.S.A.* **2006**, *103*, 11446.
- (38) Olsson, M. H. M.; Parson, W. W.; Warshel, A. *Chem. Rev.* **2006**, *106*, 1737.
- (39) Khan, A. R.; Parrish, J. C.; Fraser, M. E.; Smith, W. W.; Bartlett, P. A.; James, M. N. G. *Biochemistry* **1998**, *37*, 16839.
- (40) Moraes, T. F.; Bains, M.; Hancock, R. E. W.; Strynadka, N. C. J. *Nat. Struct. Mol. Biol.* **2007**, *14*, 85.
- (41) Denker, K.; Orlík, F.; Schiffner, B.; Benz, R. *J. Mol. Biol.* **2005**, *352*, 534.
- (42) Weiss, D.; Naik, P.; Weiss, R. *Nat. Rev. Drug Discovery* **2009**, *8*, 533.

JP9110579